Multiplexed analysis of fixed tissue RNA using Ligation *in situ* Hybridization

Joel J. Credle[1], Christopher Y. Itoh[1], Tiezheng Yuan[1], Rajni Sharma[1], Erick R. Scott[2], Rachael E. Workman[3], Yunfan Fan[3], Franck Housseau[4], Nicolas J. Llosa[4], W. Robert. Bell[5], Heather Miller[5], Sean X. Zhang[5,6], Winston Timp[3] and H. Benjamin Larman[1,*]

[1]Division of Immunology, Department of Pathology, Johns Hopkins School of Medicine, Baltimore, MD 21205, USA, [2]Department of Genetics & Genomic Sciences, Icahn Institute for Genomics and Multiscale Biology, Icahn School of Medicine at Mount Sinai, New York, NY 10078, USA, [3]Department of Biomedical Engineering, Johns Hopkins University, Baltimore, MD 21218, USA, [4]Sidney Kimmel Comprehensive Cancer Center, Department of Oncology, and the Bloomberg-Kimmel Institute for Cancer Immunotherapy, Johns Hopkins University School of Medicine, Baltimore, MD 21205, USA, [5]Division of Medical Microbiology, Department of Pathology, Johns Hopkins School of Medicine, Baltimore, MD 21287, USA and [6]Microbiology Laboratory, Johns Hopkins Hospital, Johns Hopkins Medical Institutes, Baltimore, MD 21287, USA

ABSTRACT

Clinical tissues are prepared for histological analysis and long-term storage via formalin fixation and paraffin embedding (FFPE). The FFPE process results in fragmentation and chemical modification of RNA, rendering it less suitable for analysis by techniques that rely on reverse transcription (RT) such as RT-qPCR and RNA-Seq. Here we describe a broadly applicable technique called 'Ligation *in situ* Hybridization' ('LISH'), which is an alternative methodology for the analysis of FFPE RNA. LISH utilizes the T4 RNA Ligase 2 to efficiently join adjacent chimeric RNA–DNA probe pairs hybridized *in situ* on fixed RNA target sequences. Subsequent treatment with RNase H releases RNA-templated ligation products into solution for downstream analysis. We demonstrate several unique advantages of LISH-based assays using patient-derived FFPE tissue. These include >100-plex capability, compatibility with common histochemical stains and suitability for analysis of decade-old materials and exceedingly small microdissected tissue fragments. High-throughput DNA sequencing modalities, including single molecule sequencing, can be used to analyze ligation products from complex panels of LISH probes ('LISH-seq'), which can be amplified efficiently and with negligible bias. LISH analysis of FFPE RNA is a novel methodology with broad applications that range from multiplexed gene expression analysis to the sensitive detection of infectious organisms.

INTRODUCTION

Interest in the multiplexed analysis of RNA from archival human tissues has grown immensely in recent years. Multiplexed RT-qPCR panels that measure gene expression are used to guide cancer treatment, metagenomic sequencing of biopsy materials will soon be used to diagnose infectious diseases, and there has been widespread adoption of RNA-seq and NanoString technology for the study of human tissue micro-environments (1–3). Formalin fixation and paraffin embedding (FFPE) is the most widely utilized method for preserving clinical tissue specimens, as it maintains tissue architectures, stabilizes biomolecules and is compatible with a wide variety of stains, including immunostains. Formalin fixation modifies RNA with adducts such as hydroxymethyl groups, while also crosslinking RNA to itself and to other biomolecules via methylene bridge formation. In addition, RNA fragmentation via hydrolysis typically occurs prior to and during tissue preservation, and then continues at a lower rate during storage (4–6). Standard analysis of RNA typically begins with RNA purification, followed by reverse transcription, which requires stretches of unmodified RNA and then polymerase chain reaction amplification (RT-PCR). RT-PCR is inefficient and unreliable when performed on RNA isolated from chemically fixed specimens (7–10). Traditional techniques, including quantitative real time PCR and RNA-seq, therefore suffer from reduced sensitivity and unpredictable measurement biases when compared to analysis of unfixed RNA.

---

*To whom correspondence should be addressed. Email: hlarman1@jhmi.edu

Here we introduce a novel approach for efficient and highly multiplexed measurement of specific RNA sequences in FFPE specimens, which does not require RNA purification or reverse transcription. We have previously described a probe ligation chemistry that is sensitive, specific and suitable for massively multiplexed RNA analyses (11). Here, we expand that approach to the analysis of fixed RNA. After hybridizing oligonucleotide probe pairs to adjacent sites on target RNA, T4 RNA Ligase 2 (Rnl2) is used to ligate these probes together, creating an optimal product for PCR amplification and downstream analyses (Figure 1). While the cognate substrate for Rnl2 is believed to be nicked double-stranded RNA, Rnl2 can efficiently ligate a 5′-phosphorylated DNA donor strand (here termed a '5′-phospho probe') to a 3′-diribonucleotide terminated DNA acceptor strand (here termed a '3′-diribo probe'), when these molecules are hybridized adjacent to each other on a target RNA-template (Step 2 in Figure 1). This chemistry provides the most efficient RNA-templated DNA probe ligation reaction reported to date (11). We refer to this new system of fixed RNA analysis as 'Ligation *in situ* Hybridization', or 'LISH'. Ligation products formed *in situ* may be characterized via downstream methods specific to a variety of applications.

Since Rnl2 can utilize DNA templating strands (in addition to RNA templating strands) (12), background from unwanted genomic, mitochondrial or viral DNA-templated probe set ligation may theoretically confound analysis of RNA abundance. This may be particularly relevant for very low copy mRNA targets in the presence of background DNA, which is less sensitive to formalin-induced degradation. Designing probes to target exon junctions can address this concern, but constrains probe design and is limited to intron-containing RNA molecules. In the Rnl2-based approach presented here, ligation of a 5′-phospho probe to a 3′-diribo probe produces a product with an internal diribonucleotide sequence. RNase H, a nuclease that specifically digests the RNA component of RNA–DNA hybrid helices, can therefore be used to simultaneously (i) release the desired RNA-templated ligation products into solution for downstream analysis (Figure 1i, step 3), and (ii) destroy unwanted DNA-templated ligation products (Figure 1ii, step 3). Indeed, diribonucleotide-containing ligation products hybridized to DNA are efficiently cleaved at the diribonucleotide junction by RNase H2, whereas ligation products hybridized to RNA remain intact (Figure 2A). As expected, RNase H1, which requires at least four contiguous RNA bases for cleavage (13–15), can be used to efficiently liberate RNA-templated ligation products into solution, while unwanted DNA-templated ligation products are retained in the tissue section.

MATERIALS AND METHODS

Tissues and sections

Archival or discarded surgical tissue was obtained from the Johns Hopkins Pathology Department under IRB exemption IRB00089413. Tissues were fixed in formalin for at least 48 h prior to dehydration and paraffin wax embedding. 10 μm thick sections were prepared using RNase-free precautions for standard (Plus slides; Thermo Fisher,

Waltham, MA) and laser capture microdissection (LCM) (Leica PEN-membrane) slides. FFPE blocks and sections were stored in desiccant; blocks were stored at room temperature and sections were stored at −20°C.

Ligation *in situ* hybridization (LISH)

Probe design. LISH probe pairs (3′-Diribo & 5′ Phospho probes) were designed as previously described (See reference 11) and synthesized by Integrated DNA Technologies (Coralville, IA 52241, USA). For each target RNA sequence, two non-overlapping probe pairs were designed. Probe pairs were mixed in equimolar amounts to create multiplex panels, which were aliquoted and stored at −80°C, and then diluted to a working concentration of 20 pM per probe (4× final concentration) for use in LISH assays.

LISH on Plus slides. Sections deposited on Plus slides were baked at 60°C for 1 h and deparaffinized by incubating 2× for 30 min in 95°C Trilogy buffer (Cell Marque, Rocklin, CA, USA). Sections were then rinsed 4× in ddH$_2$0 and incubated 3× for 10 min in 1×-PBS-Triton X-100 (0.1% v/v), and 2× for 5 min in pre-hybridization wash buffer (2×-SSC, 20% formamide (v/v), 0.1% tween (v/v)). A 250 μl of hybridization buffer (2×-SSC, 20% formamide (v/v), 0.2 mg/ml bovine serum albumin, 2 mM ribonucleoside vanadyl complex, 1 mg/mL *Escherichia coli* tRNA, 0.1 g/ml dextran sulfate) containing the probe panel (5 pM each probe) was applied to each section followed by incubations at 60°C for 30 min and 45°C for 2 h in a humid chamber. Slides were then washed with pre-warmed post-hybridization wash buffer (45°C, 2×-SSC, 2 mM ribonucleoside vanadyl complex, 1 mg/ml *E. coli* tRNA) and then pre-warmed 1× Rnl2 ligase buffer (37°C, 50 mM Tris-HCl, 10 mM MgCl$_2$, 5 mM dithiothreitol, 1 mM ATP). Next, sections were incubated at 37°C for 2 h with 200 μl of ligase reaction mix (1× Rnl2 ligase buffer, 1.5 U Rnl2 per μl; Qiagen, Hilden, Germany). The ligase reaction mix was carefully removed by aspiration and sections were washed in room temperature post-ligation wash buffer (2×-SSC). Ligation product was released during incubation at 37°C for 30 min in 150 μl of 1× RNase H reaction mix (50 mM Tris–HCl; pH 8.3, 75 mM KCl, 3 mM MgCl$_2$, and freshly added 10 mM dithiothreitol, 6 U RNase H; Invitrogen, Carlsbad, CA, USA). The RNase H reaction was carefully aspirated and centrifuged at 20,000 x *g* for 15 min at 4°C. The cleared supernatant was carefully collected and stored at −80°C or processed immediately. Ligation products were purified and concentrated using Oligo Clean & Concentrator columns (Zymo Research, Irvine, CA, USA) according to the manufacturer's instructions.

LISH for LCM. LISH was performed on PEN membranes using the same protocol as for Plus slides, but with the following modifications. Sections were deparaffinized and then rehydrated by incubations in Xylene-Ethanol solutions (3× for 30 s in 100% xylene, 2× for 30 s in 100% ethanol, 2× for 30 s in 95% ethanol, 30 s in 70% ethanol) and finally rinsed in ddH$_2$O four times. Next, sections were incubated with pre-warmed (37°C) pepsin (Sigma-Aldrich,
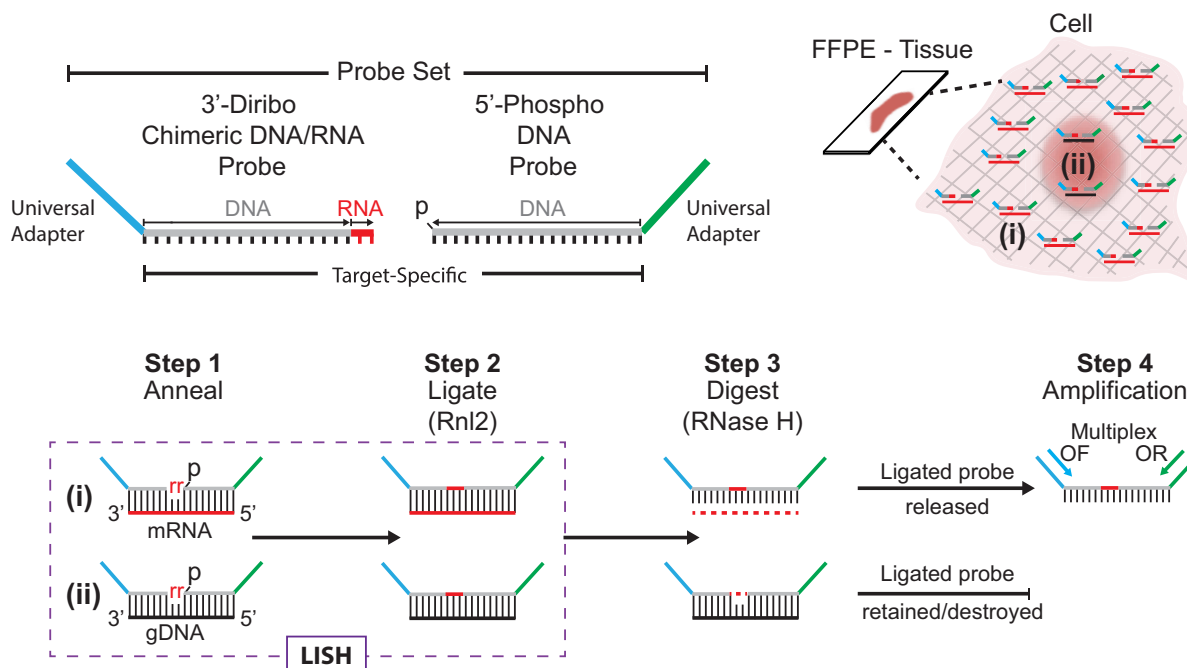
Figure 1. Workflow of the LISH assay. Step 1. Hybridization of pairs of chimeric 3′-diribonucleotide-containing and 5′-phosphorylated DNA probes on formalin fixed RNA within a tissue section. Step 2. Adjacently annealed probe pairs are then ligated *in situ* with Rnl2. Step 3. RNase H treatment (**i**) releases RNA-templated ligation products into solution for downstream analysis and (**ii**) destroys unwanted DNA-templated ligation products. Step 4. Amplification of ligation products by multiplex PCR (using universal 'outside' primers, 'OF' and 'OR').

St Louis, MO, USA) for 10 min. Sections were washed 3× in pre-hybridization buffer, incubated at 60°C for 30 min with hybridization buffer containing 5 pM of each probe and then incubated at 45°C for an additional 2 h in a humid chamber. Sections were washed with pre-warmed post-hybridization buffer and Rnl2 ligase buffer and then incubated with Rnl2 reaction mix as above. Following Rnl2 ligation of hybridized probes, sections were washed in room temperature post-ligation wash buffer as above, dried and stored in a sealed container with desiccant at room temperature until fragment collection using Leica LMD 7000 confocal microscope (Leica, Wetzlar, Germany) into 0.5 ml microcentrifuge tube caps containing 30 μl of collection buffer (1× Herculase-II reaction buffer, 5 U of Protector RNase Inhibitor; Roche, Indianapolis, IN, USA). Collected specimens were snap-frozen on dry ice followed by storage at −80°C until analyzed. Prior to pre-amplification of microdissected fragments, ligation product was thermally dissociated from fixed RNA by incubation at 95°C for 5 min, followed by a brief centrifugation step to remove insoluble material. At this point, 0.04 μl Herculase-II Fusion DNA Polymerase (Agilent, Santa Clara, CA, USA) could be added per μl reaction prior to initiation of thermal cycling.

Analysis of LISH product

End point PCR. Ligated probes were amplified in 20 μl PCR-reactions using Herculase-II following manufacturer's instructions. Temperature cycling was performed as follows: an initial denaturation step at 95°C for 2 min, followed by 20 cycles of: 95°C for 20 s, 59°C for 30 s, 72°C for 30 s, with

a final extension at 72°C for 3 min. Amplicon sizes were assessed on 3% agarose gels. PCR reactions testing different polymerases followed the manufacturers' instructions.

qPCR. qPCR analysis of LISH product followed a pre-amplification using Herculase-II Fusion DNA Polymerase (as above) for 20 cycles under normal circumstances or 30 cycles for product recovered from microdissected or extremely small specimens. Pre-amplification products were diluted 1:1,000 for qPCR analysis. 10 μl SYBR green reactions (qPCR SYBR Advantage kit; Clontech, Mountain View, CA, USA) containing probe-specific primers (see Supplementary Table S3) were analyzed on an ABI 7500 Real-Time PCR System (Halethorpe, MD, USA). Post-run melt-curve analysis was used to check amplicon purity.

Illumina sequencing. LISH products were pre-amplified as above with 20 or 30 cycles as appropriate, using the multiplex outside primers. A total of 2 μl of this product was used as input into a 20 μl indexing PCR reaction, using a standard dual-indexing strategy. Briefly, forward and reverse primers containing Illumina i7 and i5 adapters containing unique 8-mer barcodes (Additional Table S3) were used in the indexing PCR reaction for 10 cycles (Additional Figure 4). Indexed PCR products were pooled and column purified 2× (QIAquick PCR Purification Kit, Qiagen, Hilden, Germany). Libraries were sequenced using either the NextSeq 500 or the HiSeq 2500 (Illumina, La Jolla, CA, USA), with a single-end, 50-cycle protocol using a custom read 1 sequencing primer and a custom i5 sequencing primer when analyzed on the NextSeq 500 (Additional Table S3). We used an in-house python pipeline for sequence alignment and
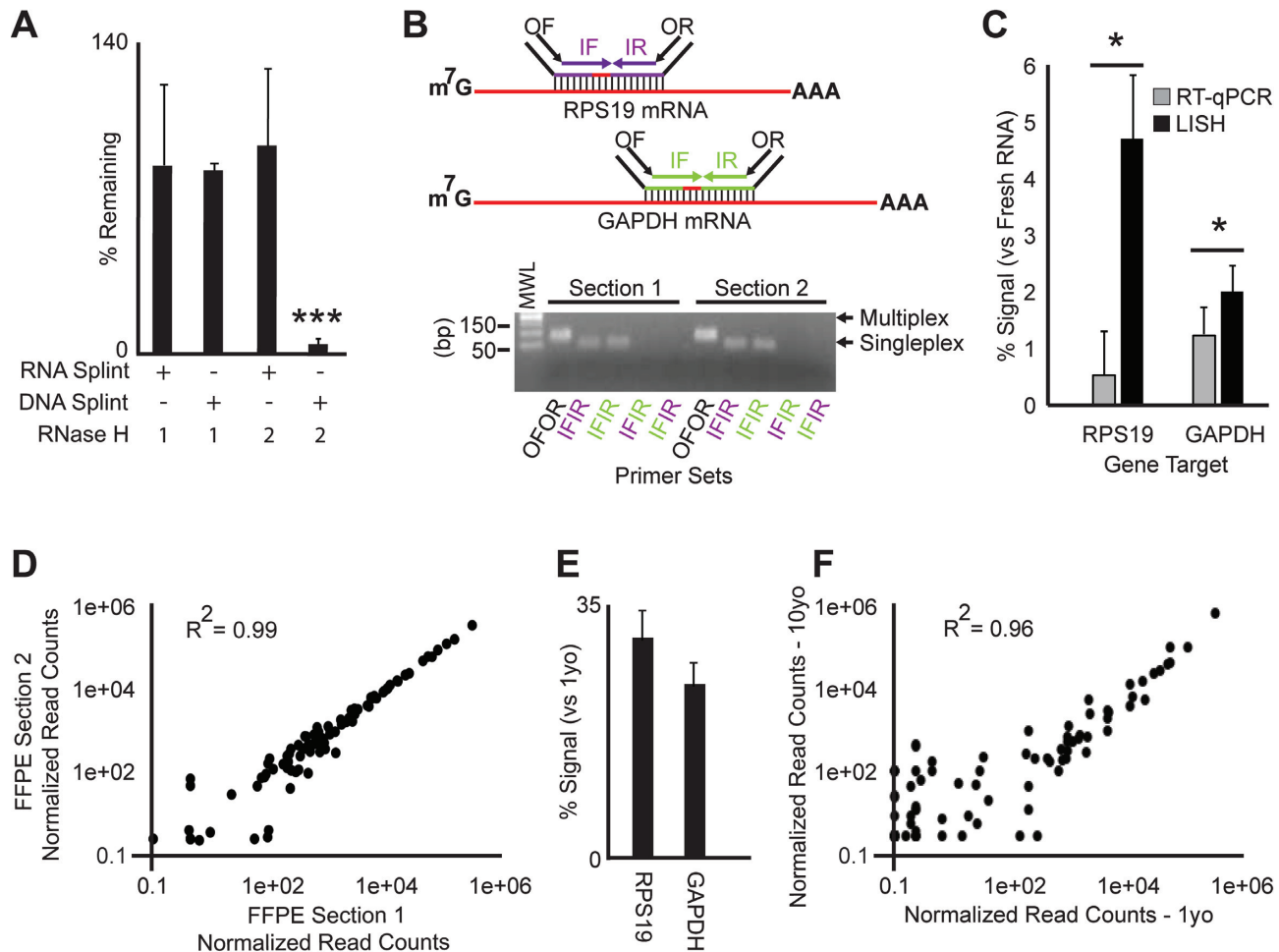
Figure 2. LISH-PCR and LISH-seq analysis of FFPE samples. (**A**) Synthetic ligation product was pre-annealed on an RNA or DNA template, followed by RNase H1 or RNase H2 digestion. Remaining ligation products were quantified by qPCR and normalized to undigested products. (**B**) Two independent LISH reactions were performed on 10 μm thick FFPE spleen tissue sections. End-point PCR analysis using multiplex 'OFOR' primers or singleplex 'IFIR' primers to detect matched and unmatched GAPDH and RPS19 probe pair ligations. Colors correspond to the target mRNA. (**C**) RPS19 and GAPDH detection efficiency using LISH versus RT-qPCR of FFPE RNA, compared with RASL or RT-qPCR analysis of fresh RNA (details in 'Materials and Methods' section). Error bars denote +/− s.d. of the mean by Student's *t*-test (A, C, $n = 3$, *$P < 0.05$, ***$P < 0.001$). (**D**) Quantification of immune panel LISH products using Illumina sequencing. Two serial sections from the same 1-year old FFPE specimen were subjected to LISH-seq. Normalized read counts are plotted for each probe set. (**E**) LISH-qPCR analysis of RPS19 and GAPDH in sections from FFPE resected tonsil tissues archived for ∼1 or ∼10 years. (**F**) LISH-seq quantification of immune panel comparing ∼1 or ∼10 years of archival storage. Sequencing reads mapped to each probe set were divided by total on-target reads for each of three sections at each archival age. The median of the normalized read counts are plotted. Error bars denote +/− s.d. of the mean.

read counting. Ligation products are 40 nt long, so the 3′ 10 nt were trimmed prior to alignment. After demultiplexing, Bowtie 2 was used to align each read against our LISH probe ligation product sequence database (using parameters '-a –best –strata -l 40 -v 2 –norc –nomaqround –samnohead'), which was composed of all possible 3′-diribo-5′phospho probe ligation products. Mismatched probe ligations (∼5% of all reads on average) were excluded from further analysis.

Nanopore sequencing. One of the *Exserohilum rostratum* libraries that had been sequenced using an Illumina instrument, was subjected to 10 rounds of additional PCR using primers containing adapters compatible with the MinION nanopore sequencing platform (Oxford Nanopore; Supplementary Table S3). This PCR product was column purified

(QIAquick PCR Purification Kit). A second round of PCR (OneTaq, NEB) adding Oxford-specific barcodes was performed, allowing us to multiplex (although we chose not to in this case). PCR product was purified using Ampure XP (Agencourt), and quantified using a Qubit dsDNA HS Assay kit (Thermo Fisher). A total of 500 ng of PCR-product was then A-tailed (NEB), cleaned using Ampure, quantified and diluted to 0.2 pmols (220 bp average length). Ligation of hairpin and leader adapters (Oxford Nanopore Genomic DNA Sequencing Kit NSK-007) was performed using Blunt/TA ligase master mix (NEB) and was followed by attachment of a biotinylated tether molecule, which when bound specifically to the hairpin adapter, is enriched for using a Streptavidin bead pull-down (Dynabeads MyOne C1). Prepared libraries were sequenced on an R9 flowcell for 48 h. For analysis, we extracted the fasta sequences and times-

tamps of the reads with poretools blasted against the known sequences for on- and off-target *E. rostratum* probes (16). Cumulative distribution plots of the number of reads for each probe versus the read completion time were plotted with a custom R script.

LISH versus RT-qPCR analysis. PureLink FFPE mRNA kit (Thermo Fisher, Waltham, MA, USA) was used to purify total RNA according to manufacturer's instructions, with slight modifications. A single 10 μm thick section was used per purification. RNA was eluted in 30 μl of RNase-free water. RNA concentration, purity and quality were determined by NanoDrop (Thermo-Fisher, Waltham, MA, USA) and Bioanalyzer (Agilent, Santa Clara, CA, USA). RNA was converted into cDNA using the Superscript-III kit (Invitrogen, Carlsbad, CA, USA) following manufacturer's instructions with the following modifications. mRNA (derived from fresh or fixed samples) was first immobilized on oligo-dT magnetic beads (M1 Dynabeads, Invitrogen). These beads were used as input to the RT reaction. This allowed us to compute the relative effect of fixation on RT-qPCR analysis of FFPE-derived splenic RNA (by comparison with RT-qPCR analysis of fresh splenic RNA; Human Spleen Total RNA, Agilent, Cedar Creek, TX, USA), versus the relative efficiency of LISH analysis of FFPE splenic RNA *in situ* (by comparison with RASL analysis of fresh splenic RNA). The mass of the RNA input into the qPCR and RASL assays was the same, and the amount of RNA in the LISH sections were approximated by the yield of the RNA purification using the PureLink FFPE kit. For the RT-qPCR versus LISH analysis, the same 'inside' singleplex PCR primers were used to pre-amplify and then quantify both the RT products (cDNA) and the corresponding LISH ligation products.

Histochemical and immunohistochemical staining

The following tissue staining methods (H&E, Cresyl Violet and IHC) used suggested protocols for maintaining RNA integrity (17). Calcofluor white (CW) and periodic acid-Shiff (PAS) staining used manufacturer's suggested protocols (Sigma-Aldrich, Indianapolis, IN, USA) with the following modifications. Addition of KOH was omitted from the CW staining procedure. For immunohistochemistry (IHC), Protector RNase Inhibitor (5U in 100 μl) was added to each step. Following staining, sections were dried and stored in a sealed container with desiccant until imaging or LISH analysis. Images were acquired under RNase-free conditions using an Olympus CX22 microscope (Olympus, Central Valley, PA, USA) at 20 and 40× magnification or for fluorescence imaging, acquired with a Zeiss LMCF Axio epifluorescence microscope at 20 and 40× magnification.

Statistical analysis

All results are expressed as mean ± standard deviation with significance determined by Student's *t*-test (*$P < 0.05$, ***$P < 0.001$).

RESULTS

We first assessed whether or not FFPE RNA could serve as a suitable template for Rnl2-mediated probe ligation *in situ*. Probe pairs targeting the GAPDH and RPS19 housekeeping genes were used to assay a 10 micron thick FFPE section of surgically resected human spleen, a tissue particularly prone to RNA degradation (18,19). End-point PCR analysis of the RNase H released ligation products ('LISH-PCR') revealed that the correct probe pairs were indeed ligated *in situ*, whereas target-mismatched probe pairs were not ligated at detectable levels (Figure 2B and Additional Figure 1A–C). To quantify the amount of specific ligation products formed during a multiplexed LISH reaction, we developed qPCR assays for each of the four possible ligation products ('LISH-qPCR'; two target-matched, or 'on-target', products and two target-mismatched, or 'off-target', products). These assays were then used to determine the amount of signal (on-target probe ligation) to noise (off-target probe ligation), while various LISH protocol parameters were optimized (Additional Figure 1D and E). We next sought to establish the relative efficiency of LISH compared to RT-qPCR analysis of RNA purified from fixed or unfixed tissue samples. LISH-based detection of GAPDH was 1.6-fold more efficient than RT-qPCR analysis of the same RNA ($P = 0.05$; Figure 2C), while LISH-based detection of RPS19 was ∼9-fold more efficient than RT-qPCR analysis of the same RNA ($P = 0.01$; Figure 2C). These data indicate that LISH may be a more sensitive technique for detecting and quantifying RNA sequences in FFPE tissues, compared with RT-based analyses of purified FFPE RNA.

Vast clinical archives of FFPE specimens are invaluable, yet underutilized resources of human tissues. A method to recover high quality transcriptional information from archived tissues would therefore be of great utility, particularly for the investigation of limited or rare patient specimens. We retrieved FFPE tonsil tissue blocks from surgical resections performed ∼1 or ∼10 years ago to assess assay reproducibility and the effects of specimen age on LISH performance. Ten micron thick sections were cut from each specimen and assayed by LISH using a panel of 97 housekeeping and immune-related probe pairs (Additional Table S1) (20). The recovered ligation product was amplified and quantified by Illumina sequencing ('LISH-seq'). Two serial sections from the same 1-year old FFPE specimen were independently assayed by LISH-seq and found to be in excellent agreement (Pearson $R^2 = 0.99$; Figure 2D). The percentage of sequencing reads mapped to correctly paired probe sets averaged 95% for both sections. While the absolute amount of ligation product was reduced, as expected, in the 10-year old specimens (Figure 2E), the relative gene expression profile determined by LISH was well preserved over this time period (Pearson $R^2 = 0.96$; Figure 2F).

An additional benefit of using RNase H for LISH product retrieval is that untargeted tissue RNA molecules should remain undigested, and thus available for subsequent analyses. This feature may be useful for investigations of limiting specimens, particularly in the case that a first LISH analysis may indicate a second, non-overlapping LISH analysis. To assess the performance of sequential LISH assays, we constructed two non-overlapping probe pools, which could
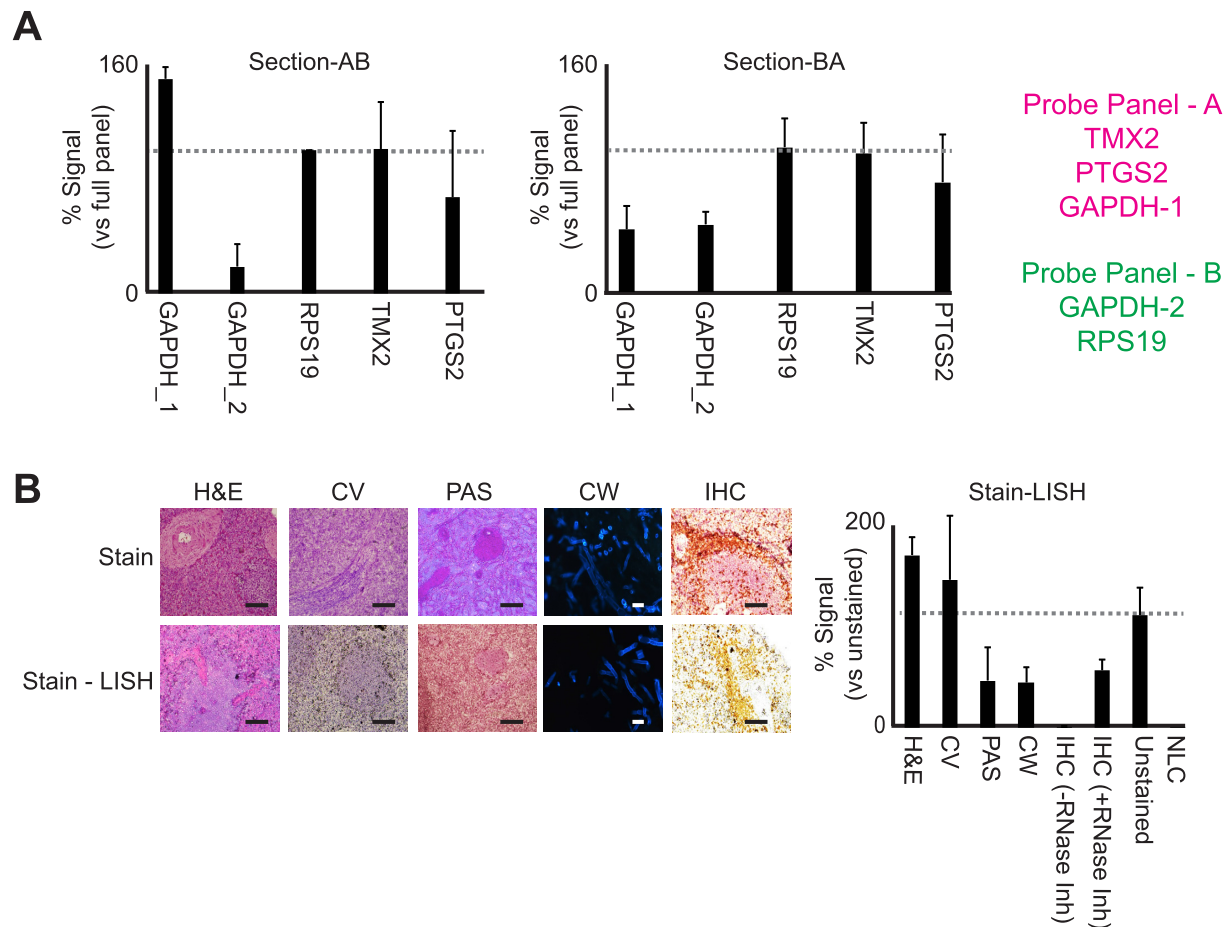
Figure 3. The LISH assay is non-destructive and compatible with common histological stains. (**A**) LISH-qPCR was performed twice on the same FFPE sections using two non-overlapping probe pools (Panel-A or Panel-B) in opposite order. Panel-A was measured after LISH-1 on section AB and after LISH-2 on section BA. Panel-B was measured after LISH-1 on section BA and after LISH-2 on section AB. (**B**) Hematoxylin and Eosin (H&E), Cresyl Violet (CV), Periodic Acid Schiff (PAS), Calcofluor White (CW) and α-CD3 Immunohistochemical Staining (IHC) were used prior to performing LISH. qPCR analysis of RPS19 probe ligation product was used to measure loss of signal due to staining, by comparison with an unstained section. Scale bar (100 μm for H&E, CV, PAS and IHC) and (50 μm for CW). Error bars denote +/− s.d. of the mean.

be used in parallel on separate FFPE sections, but in opposite order (see Additional Figure 2A and B for experimental design). Two sequential LISH assays were performed with these probe sets on two sequential days. Ligation products from probes targeting distinct transcripts (e.g. RPS19 versus GAPDH) were minimally reduced (∼5% to ∼30%; Figure 3A). Ligation products from probes targeting the same transcript (GAPDH_1 versus GAPDH_2), however, were reduced much more significantly (∼55% to ∼80%). This suggests that probe panels used for sequential LISH analyses should avoid targeting the same RNA molecules. Notably, carryover signal from the first round of LISH was nearly undetectable, consistent with complete product retrieval using RNase H.

Pathologists utilize a rich diversity of histochemical stains to characterize FFPE sections. Many of these, particularly hematoxylin and eosin (H&E) and immunohistochemistry (IHC), would be useful to combine with LISH, for example to guide analysis of specific tissue regions of interest. We reasoned that stains, which do not completely destroy the RNA content of the section would be compat-

ible with subsequent LISH analysis. To test this, we challenged the tissue with several histological stains prior to performing LISH. LISH-qPCR was then used to assess the abundance of RPS19 ligation product (Figure 3B). RPS19 yield varied by stain but was generally acceptable with at most an ∼3-fold loss. H&E and CV staining had little effect on RPS19 signal, whereas PAS, CW and IHC reduced signals by ∼2- to 3-fold compared to the unstained control. Notably, when RNase inhibitor was absent from the IHC buffers (which included serum-derived primary antibody) the RPS19 ligation product was undetectable (Figure 3B), providing evidence that the LISH-qPCR signal from unwanted gDNA-templated probe ligation is below the level of detection (>1000-fold lower than the signal from RNA-templated probe ligation). These data highlight the general compatibility of tissue staining followed by LISH analysis, whenever RNA integrity is sufficiently preserved. Importantly, performing LISH after staining did not interfere with visualization of morphological features.

A reliable method for highly multiplexed gene expression analysis of extremely small tissue fragments, such as
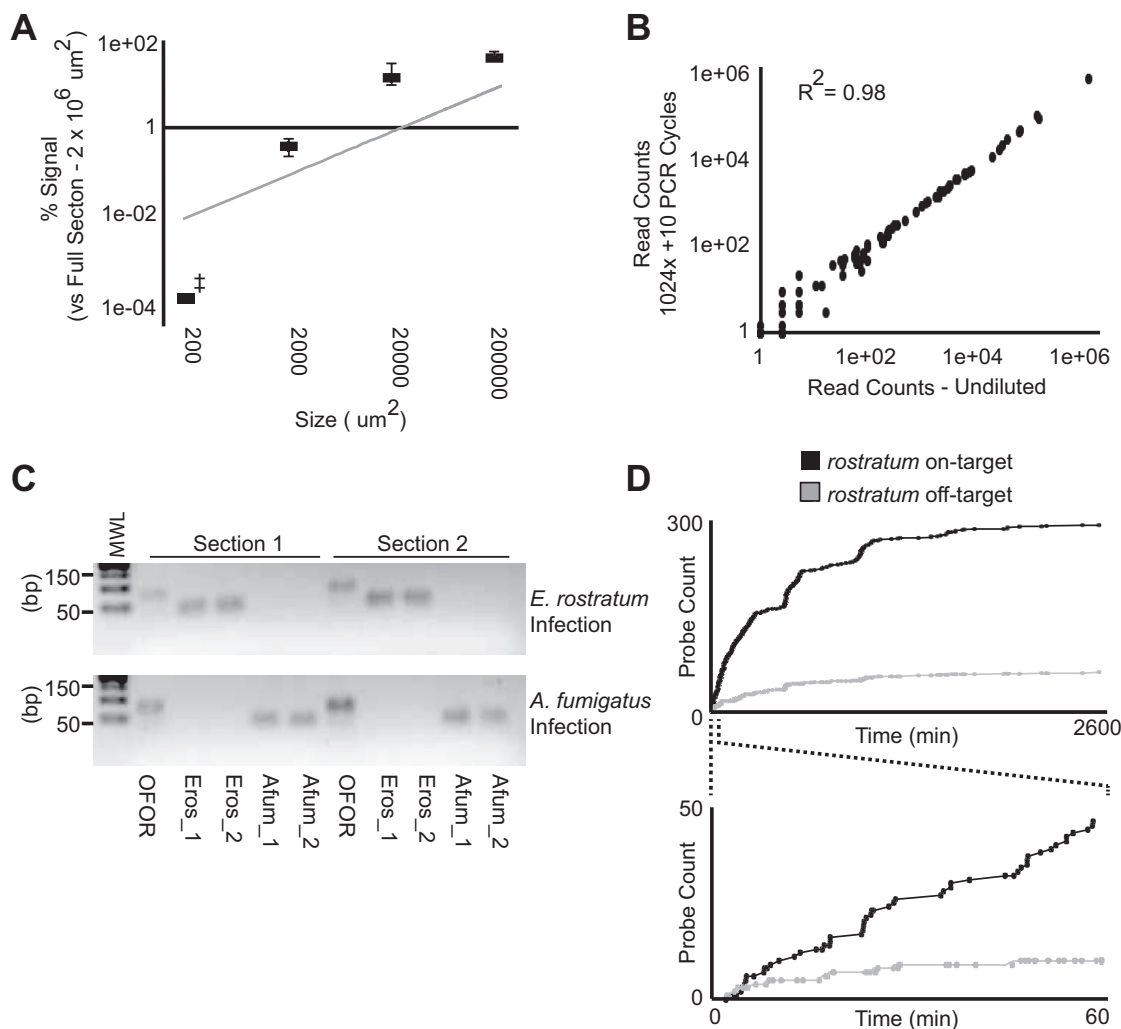
Figure 4. LISH sensitivity and its use in clinical diagnosis. (**A**). LISH-qPCR was used to measure RPS19 expression in tissue fragments obtained by LCM. Signal is reported as percentage versus LISH-qPCR from a full, serial FFPE section ($\sim 1 \times 10^6$ μm^2). Gray line indicates expected signal, based on the area of an LCM fragment. ‡ For the 67 μm^2 LCM fragments, data from qPCR reactions that did not give signal greater than the no ligase control (4 of 6) were excluded from this analysis. (**B**) Multiplex LISH-PCR product was diluted 1024-fold and subjected to 10 additional cycles of multiplex PCR. Illumina sequencing was then used to quantify each ligated probe set. Normalized read counts are plotted. (**C**) End point LISH-PCR from a fungal species-specific LISH probe panel. Two FFPE sections from a brain biopsy positive for *E. rostratum*, and two from a brain biopsy positive for *Aspergillus fumigatus* were analyzed with the pool. Outside primers (OFOR) or inside primers (e.g. Eros_1, Eros_2, Afum_1, Afum_2) were used for the PCR. (**D**) Multiplex amplicon from the LISH fungal panel assay performed on the *E. rostratum* positive biopsy was analyzed using the Oxford Nanopore MinION DNA sequencer. Cumulative Eros_1/2 on-target reads are plotted versus the cumulative off-target reads as a function of time. The top graph displays data collected during the entire run; the bottom graph displays data collected over the first hour of the run. Error bars denote +/− s.d. of the mean.

those obtained by LCM, would be of great value for linking gene expression patterns with positional information. LISH probe pair ligation products are short and uniform in size, and are thus optimal for efficient amplification with minimal bias. Also advantageous is that entire sections can be uniformly hybridized and ligated prior to microdissecting multiple regions of interest for comparison (21,22). We therefore examined the performance of LISH in the context of decreasing LCM fragment size. From a 10 micron thick FFPE spleen section, we performed LISH and then used LCM to obtain a series of fragments ranging from 6.7×10^4 μm^2 down to ~ 67 μm^2 (the equivalent of ~ 1000 down to ~ 1 cross sectional cell areas, respectively). Tissue fragments underwent multiplex PCR amplification using the universal PCR adapters, followed by qPCR quantification of RPS19

probe ligation products. The result was a reliable signal in direct proportion to LCM fragment size, and roughly equivalent to the expected magnitude (Figure 4A). From even the smallest 67 μm^2 fragments, we observed signal-to-noise ratios of up to >16, compared with negative control reactions (no ligase). We next examined the extent to which PCR amplification bias might distort relative quantification of each ligated probe pair. To this end, the products of a multiplexed LISH-PCR reaction were diluted 2^{10}-fold and then PCR amplified for an additional 10 cycles. These amplicons were then separately indexed and Illumina sequenced for quantitation. Based on the observed read counts, negligible skewing occurred during the $\sim 10^3$-fold amplification (Pearson $R^2 = 0.99$; Figure 4B), suggesting that the relative abundance of LISH products is tightly maintained during

PCR amplification. Reliable recovery from small LCM fragments, together with undistorted PCR amplification make LISH an ideal technique for highly multiplexed gene expression measurement of microscopic tissue structures.

A high sensitivity technique for detecting a large number of RNA sequences in FFPE specimens would be useful for the detection of infectious organisms. In clinical mycology, for example, chemical stains often reveal the presence of a fungal organism, but accurate taxonomic specification can be elusive. This was the case in 2012 during an outbreak of a mysterious fungal meningitis, which was later traced to contaminated methylprednisone injections (23,24). Of the 745 cases, only 14% had a positive culture and ∼50% could be confirmed by PCR (25,26). We obtained a small FFPE brain biopsy from one case (27) (Additional Figure 3A), and performed multiplexed LISH using a panel of six probe pairs designed to distinguish among three closely related clinically relevant fungal species (Additional Table S2). The *Exserohilum rostratum* detector probes reported strong on-target signal from the patient treated with contaminated methylprednisone, but not from biopsies of uninfected tissues or brain sections containing unrelated but common fungal infections, such as *Aspergillus fumigatus* (Figure 4C, Additional Figure 3B). Multiplexed LISH can therefore be used to quantify RNA from infectious organisms preserved within FFPE clinical specimens.

High throughput DNA sequencing could be used to analyze ligation products from complex panels of LISH probes designed to detect an extensive array of infectious agents. However, turnaround time and high equipment costs associated with 'next generation' DNA sequencing platforms may limit the utility of LISH-based diagnosis in the clinical setting. Compatibility with real-time, single molecule ('third generation') sequencing using relatively inexpensive equipment would therefore be of interest. We assessed the ability of Oxford Nanopore's MinION DNA sequencer to detect ligation products from the *E. rostratum* case. After only one hour of sequencing time, on-target *E. rostratum* probe ligation products had been detected at a rate of >4-fold greater than the off-target, mismatched probe pair ligation products (Figure 4D). Emerging DNA sequencing platforms may therefore enable rapid LISH-based diagnosis of infectious disease in the clinical setting at a cost far below that required for unbiased metagenomic analyses.

DISCUSSION

LISH is a novel probe-based technique for highly multiplexed measurement of RNA sequences in fixed tissue sections, which does not require RNA extraction or reverse transcription. In our investigation of its unique features, we have found the absolute sensitivity of LISH to compare favorably with RT-qPCR and that expression signatures are stable over at least a decade of sample archiving under ambient conditions. Its non-destructive nature, compatibility with various routine tissue stains and suitability for analyzing microdissected tissue fragments exemplify the versatility of LISH-based assays. In addition, LISH does not require expertise or specialized instrumentation, and could therefore be readily integrated into existing research or clinical pathology workflows. More generally, the Rnl2-based *in situ*

ligation of chimeric probes will likely have applications beyond those presented here. For example, LISH may be combined with *in situ* methods such as hybridization chain reaction for spatially resolved RNA localization (28). LISH analysis of fixed and permeabilized lymphocytes may facilitate gene expression analysis of sorted single cells or cell populations. In the context of high-throughput chemical or genetic screening, miniaturized LISH could be performed on fixed cell cultures in microtiter wells, perhaps in combination with phenotypic analyses. Finally, the ability to efficiently template the ligation of DNA probes directly on fixed RNA *in situ* may facilitate emerging technologies such as FISSEQ, (29,30), PLAYR, (31) or MERFISH (32), or others not contemplated here. For these reasons, LISH is a promising new methodology for biomedical researchers and pathologists.

SUPPLEMENTARY DATA

Supplementary Data are available at NAR Online.

REFERENCES

1. Sparano,J.A., Gray,R.J., Makower,D.F., Pritchard,K.I., Albain,K.S., Hayes,D.F., Geyer,C.E. Jr, Dees,E.C., Perez,E.A., Olson,J.A. Jr *et al.* (2015) Prospective validation of a 21-gene expression assay in breast cancer. *N. Engl. J. Med.*, **373**, 2005–2014.
2. Meyerson,M., Gabriel,S. and Getz,G. (2010) Advances in understanding cancer genomes through second-generation sequencing. *Nat. Rev. Genet.*, **11**, 685–696.
3. Beard,R.E., Abate-Daga,D., Rosati,S.F., Zheng,Z., Wunderlich,J.R., Rosenberg,S.A. and Morgan,R.A. (2013) Gene expression profiling using nanostring digital RNA counting to identify potential target

antigens for melanoma immunotherapy. *Clin. Cancer Res.*, **19**, 4941–4950.

4. Masuda,N., Ohnishi,T., Kawamoto,S., Monden,M. and Okubo,K. (1999) Analysis of chemical modification of RNA from formalin-fixed samples and optimization of molecular biology applications for such samples. *Nucleic Acids Res.*, **27**, 4436–4443.

5. Nolan,T., Hands,R.E. and Bustin,S.A. (2006) Quantification of mRNA using real-time RT-PCR. *Nat. Protoc.*, **1**, 1559–1582.

6. Gilbert,M.T.P., Haselkorn,T., Bunce,M., Sanchez,J.J., Lucas,S.B., Jewell,L.D., Van Marck,E. and Worobey,M. (2007) The isolation of nucleic acids from fixed, paraffin-embedded tissues–which methods are useful when? *PLoS One*, **2**, e537.

7. Zeka,F., Vanderheyden,K., De Smet,E., Cuvelier,C.A., Mestdagh,P. and Vandesompele,J. (2016) Straightforward and sensitive RT-qPCR based gene expression analysis of FFPE samples. *Sci. Rep.*, **6**, 21418.

8. Cronin,M., Pho,M., Dutta,D., Stephans,J.C., Shak,S., Kiefer,M.C., Esteban,J.M. and Baker,J.B. (2004) Measurement of gene expression in archival paraffin-embedded tissues: development and performance of a 92-gene reverse transcriptase-polymerase chain reaction assay. *Am. J. Pathol.*, **164**, 35–42.

9. Godfrey,T.E., Kim,S.-H., Chavira,M., Ruff,D.W., Warren,R.S., Gray,J.W. and Jensen,R.H. (2000) Quantitative mRNA expression analysis from formalin-fixed, paraffin-embedded tissues using 5′ nuclease quantitative reverse transcription-polymerase chain reaction. *J. Mol. Diagn.*, **2**, 84–91.

10. Chung,J.-Y., Braunschweig,T. and Hewitt,S.M. (2006) Optimization of recovery of RNA from formalin-fixed, paraffin-embedded tissue. *Diagn. Mol. Pathol.*, **15**, 229–236.

11. Larman,H.B., Scott,E.R., Wogan,M., Oliveira,G., Torkamani,A. and Schultz,P.G. (2014) Sensitive, multiplex and direct quantification of RNA sequences using a modified RASL assay. *Nucleic Acids Res.*, **42**, 9146–9157.

12. Nandakumar,J. and Shuman,S. (2004) How an RNA ligase discriminates RNA versus DNA damage. *Mol. Cell*, **16**, 211–221.

13. Nowotny,M., Gaidamakov,S.A., Ghirlando,R., Cerritelli,S.M., Crouch,R.J. and Yang,W. (2007) Structure of human RNase H1 complexed with an RNA/DNA hybrid: insight into HIV reverse transcription. *Mol. Cell*, **28**, 264–276.

14. Eder,P.S., Walder,R.Y. and Walder,J.A. (1993) Substrate specificity of human RNase H1 and its role in excision repair of ribose residues misincorporated in DNA. *Biochimie*, **75**, 123–126.

15. Hiller,B., Achleitner,M., Glage,S., Naumann,R., Behrendt,R. and Roers,A. (2012) Mammalian RNase H2 removes ribonucleotides from DNA to maintain genome integrity. *J. Exp. Med.*, **209**, 1419–1426.

16. Loman,N.J. and Quinlan,A.R. (2014) Poretools: a toolkit for analyzing nanopore sequence data. *Bioinformatics*, **30**, 3399–3401.

17. Leica Inc (2011) Sample preparation for laser capture microdissection. http://www.leica-microsystems.com/products/light-microscopes/life-science-research/laser-microdissection/.

18. Fleige,S., Walf,V., Huch,S., Prgomet,C., Sehm,J. and Pfaffl,M.W. (2006) Comparison of relative mRNA quantification models and the impact of RNA integrity in quantitative real-time RT-PCR. *Biotechnol. Lett.*, **28**, 1601–1613.

19. Jewell,S.D., Srinivasan,M., McCart,L.M., Williams,N., Grizzle,W.H., LiVolsi,V., MacLennan,G. and Sedmak,D.D. (2002) Analysis of the molecular quality of human tissues: an experience from the Cooperative Human Tissue Network. *Am. J. Clin. Pathol.*, **118**, 733–741.

20. Llosa,N.J., Cruise,M., Tam,A., Wicks,E.C., Hechenbleikner,E.M., Taube,J.M., Blosser,R.L., Fan,H., Wang,H., Luber,B.S. *et al.* (2015) The vigorous immune microenvironment of microsatellite instable colon cancer is balanced by multiple counter-inhibitory checkpoints. *Cancer Discov.*, **5**, 43–51.

21. Quail,D.F. and Joyce,J.A. (2013) Microenvironmental regulation of tumor progression and metastasis. *Nat. Med.*, **19**, 1423–1437.

22. Junttila,M.R. and de Sauvage,F.J. (2013) Influence of tumour micro-environment heterogeneity on therapeutic response. *Nature*, **501**, 346–354.

23. Kainer,M.A., Reagan,D.R., Nguyen,D.B., Wiese,A.D., Wise,M.E., Ward,J., Park,B.J., Kanago,M.L., Baumblatt,J. and Schaefer,M.K. (2012) Fungal infections associated with contaminated methylprednisolone in Tennessee. *N. Engl. J. Med.*, **367**, 2194–2203.

24. Smith,R.M., Schaefer,M.K., Kainer,M.A., Wise,M., Finks,J., Duvve,J., Fontaine,E., Chu,A., Carothers,B. and Reilly,A. (2013) Fungal infections associated with contaminated methylprednisolone injections. *N. Engl. J. Med.*, **369**, 1598–1609.

25. Feldmesser,M. (2013) Fungal disease following contaminated steroid injections: exserohilum is ready for its close-up. *Am. J. Pathol.*, **6**, 661–664.

26. Ritter,J.M., Muehlenbachs,A., Blau,D.M., Paddock,C.D., Shieh,W.J., Drew,C.P., Batten,B.C., Bartlett,J.H., Metcalfe,M.G., Pham,C.D. *et al.* (2013) Exserohilum infections associated with contaminated steroid injections: a clinicopathologic review of 40 cases. *Am. J. Pathol.*, **6**, 881–892.

27. Bell,W.R., Dalton,J.B., McCall,C.M., Karram,S., Pearce,D.T., Memon,W., Lee,R., Carroll,K.C., Lyons,J.L. and Gireesh,E.D. (2013) Iatrogenic Exserohilum infection of the central nervous system: mycological identification and histopathological findings. *Mod. Pathol.*, **26**, 166–170.

28. Dirks,R.M. and Pierce,N.A. (2004) Triggered amplification by hybridization chain reaction. *Proc. Natl. Acad. Sci. U.S.A.*, **101**, 15275–15278.

29. Lee,J.H., Daugharthy,E.R., Scheiman,J., Kalhor,R., Yang,J.L., Ferrante,T.C., Terry,R., Jeanty,S.S., Li,C., Amamoto,R. *et al.* (2014) Highly multiplexed subcellular RNA sequencing in situ. *Science*, **343**, 1360–1363.

30. Lee,J.H., Daugharthy,E.R., Scheiman,J., Kalhor,R., Ferrante,T.C., Terry,R., Turczyk,B.M., Yang,J.L., Lee,H.S., Aach,J. *et al.* (2015) Fluorescent in situ sequencing (FISSEQ) of RNA for gene expression profiling in intact cells and tissues. *Nat. Protoc.*, **10**, 442–458.

31. Frei,A.P., Bava,F.-A., Zunder,E.R., Hsieh,E.W., Chen,S.-Y., Nolan,G.P. and Gherardini,P.F. (2016) Highly multiplexed simultaneous detection of RNAs and proteins in single cells. *Nat. Methods*, **13**, 269–275.

32. Chen,K.H., Boettiger,A.N., Moffitt,J.R., Wang,S. and Zhuang,X. (2015) RNA imaging. Spatially resolved, highly multiplexed RNA profiling in single cells. *Science*, **348**, aaa6090.